A machine learning based Bayesian decision support system for efficient navigation of double-ended ferries

Journal of Ocean Engineering and Science xxx (xxxx) xxx

Contents lists available at ScienceDirect

Journal of Ocean Engineering and Science

journal homepage: www.elsevier.com/locate/joes

Research Paper

A machine learning based Bayesian decision support system for efficient navigation of double-ended ferries

Vergara Daniel[a], Alexandersson Martin[a,b], Lang Xiao[a], Mao Wengang[a,*]

[a] Department of Mechanics and Maritime Sciences, Chalmers University of Technology, Sweden
[b] SSPA, Research Institutes of Sweden, Gothenburg, Sweden

ARTICLE INFO

Article history:
Received 21 June 2023
Revised 18 September 2023
Accepted 8 November 2023
Available online xxx

Keywords:
Bayesian optimization
Energy efficiency
Ship navigation
Machine learning ship models

ABSTRACT

Ships can be operated more efficiently by utilizing intelligent decision support integrated with onboard data collection systems. In this study, a Bayesian optimization-based decision support system, which utilizes ship performance models built by machine learning methods, is proposed to help determine the operational set-points of two engines for double-ended ferries. By optimizing the ferries' power allocation between the stern and bow engines, the Decision Support System (DSS) will simultaneously attempt to keep the ETA of the ferry fixed under a set of operational constraints using the Bayesian optimization. Its objective is to minimize fuel consumption along individual trips. Based on simulation environment, the DSS can reduce at maximum 40 % fuel consumption with no significant change of the ETA. Final full-scale experiments of a double-ended ferry demonstrated an average of 15 %, where at least half of this saving was achieved by the optimized power allocation between bow and stern engines.

1. Introduction

The shipping industry is keen to reduce fuel consumption and air emissions [1]. Some operation related energy efficiency measures can be straightforwardly implemented to increase shipping sustainability [2], such as voyage optimization [3,4], speed management [5]and performance monitoring [6–12]. For short-sea shipping and with critical requirements on ETA (expected time of arrival), there are only marginal spaces for the speed and voyage optimization. Especially in the cases of doubleended ferries often used as commuter vessels between islands for their good manoeuvrability [13], their actual operational performance is not well known to the operators, because of their two sets of propulsion systems, one at the stern and one at the bow. Even though basic ship principles tell that a configuration with all the power allocated in the stern propeller can result in the maximum efficiency [14], they also indicate very small difference of total fuel consumption due to different power allocation between the two propellers. Therefore, it was observed in [15] that ship operators arbitrarily set power allocations to operate their ferries. As the development of shipping digitalization, collected data onboard ships clearly show that there are large fuel saving potentials by setting better configuration of power allocations for those double ended ferries [15]. But optimal configurations require knowledge beyond the master mariners' capabilities, therefore some Decision Support System will be greatly beneficial for ship operators to navigate their ships more environmentally friendly.

Some decision support systems were developed for those double-ended ferries but mainly for the Manoeuvring study and autonomous navigation [16,17]. While design support tools/algorithms were also well researched for reducing emissions from shipping based on ship performance simulations [18,19]. For double ended ferries, their actual ship performance is rarely researched and current semi-empirical ship performance models [20–22] may not accurately describe those ferries' energy performance for developing DSS. In recent maritime research, the adoption of machine learning techniques has been recognized for its potential to optimize ship operations for energy efficiency. Machine learning models have been developed that accurately capture a ship's performance in the actual sailing. Through these models, ship speed can be meticulously predicted [23–26], and insights into fuel consumption can be provided [7,27–30]. Based on these models, ship speed can be strategically managed, and enhanced operational efficiency can be realized [31–34].

In this study, a machine learning algorithm is utilized to build such a performance model for the double-ended ferry. The established data-driven model will be integrated into the Bayesian optimization algorithm. They can simulate the ferry's performance

* Corresponding author.
E-mail address: wengang.mao@chalmers.se (M. Wengang).

https://doi.org/10.1016/j.joes.2023.11.002

Nomenclature

DSS	Decision Support System
ETA [min]	Estimated Time of Arrival
T_s [min]	Sailing Time
V_g [kts]	Speed Overground
FCR	Fuel Consumption Rate
m [l/s]	FCR Engine
L [%]	Engine's Load
P [kW]	Engine's Power
n [rpm]	Engine's speed
V_{wr} [kts]	Relative Wind Speed
ϕ_{wr} [deg]	Relative Wind Angle
V_{sc} [m/s]	Sea Current Speed
ϕ_{sc} [deg]	Sea Current Angle
R_p	Power Ratio
X_s	Associated to ship's stern
X_b	Associated to ship's bow
$f(-)$	Generic function
X^*	Optimum
$\bar{X}$	Mean value of X
m [l]	Fuel Consumption
$J(-)$	Objective Function
q [%]	Relative tolerance
ξ	Control inputs
$K(\xi)$	Kernel Function of ξ
$k(\xi)$	Augmentation row for K
ΔV_g	Relative Tolerance of Speed
ΔR_p	Relative Tolerance of Rp
GP	Gaussian Process
$\alpha(-)$	GP Acquisition Function
$\mu(-)$	GP Mean Function
$\sigma(-)$	GP Standard Deviation Function
a	Z-score for a given confidence.

to formulate an onboard decision support system, which can provide real-time optimal configuration of engine settings for both bow and stern propellers. The objective of the DSS is setup for minimum fuel consumption along each trip also keep its ETA. For the completeness of this paper, Section 2 presents brief information regarding the challenges of double-ended ferry optimal operations, using a case study ferry. The methods for the proposed DSS are presented in Section 3. And Section 4 presents results of fuel savings by the proposed DSS for both simulation environments and full-scale test environments.

2. Challenge of double-ended ferry operations

In modern ships, captains can issue a command from the ship bridge directly into the engine through the throttle control, which is a lever or handle with different positions that regulates the amount of fuel injection into the compression-ignition cylinders. The fuel intake controls the engine's speed and load and power outputs. The double-ended ferry command bridge has two throttle levers, one for each engine. Therefore, finding the optimal control strategy of engines to reduce ship total fuel consumption becomes more difficult. A basic sketch of such a double-ended vessel is illustrated in Fig.1. The main engine notations (Engine 1 and Engine 2) will switch their functionalities between stern and bow engines for different trip directions. For the sake of convenience, bow and stern engines are used for the description. Table 1 enumerates the critical operational parameters pertinent to double-ended ferries. These parameters were judiciously selected, grounded in the well-established foundational principles of ship propulsion. It is acknowledged that the rate of fuel consumption (represented as m) is correlated to both the vessel's speed (V_g) and the engine's rotational speed (n). Environmental factors, including wind, waves, and currents, further compound the influence on fuel consumption [35].

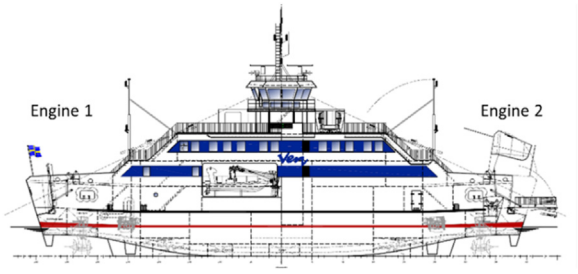

Fig. 1. General arrangement of a double-ended ferry.

Fig. 2. Routes collected for one year's sailing of this case study double-ended ferry used in this study.

For optimal navigation of such double-ended ferries, one of the big challenges is to understand the ferry's performance in terms of different engine settings. Reliable models are rarely available, and there are not mature enough guidelines to assist actual navigation of those ferries. As the increase of shipping digitalization, some data collection systems can be easily installed onboard those ferries to assist development of the DSS for energy efficient operations. In the following, a case study double-ended ferry with data collections onboard is used to demonstrate the challenges and validate the proposed DSS.

2.1. Case study double-ended ferry

The case study is a RoRo passenger ship named Uraniborg with a ship length 46 m, service speed 11.5 knots, and two identical internal combustion engines Caterpillar C32 ACERT V12 with maximum rating 709 kW of 1600 rpm. The ferry transits the Øresund, specifically the route Ven-Landskrona in southern Sweden, a route that is approximately 4 nautical miles as shown in Fig. 2. It is a commuter ferry that goes 18 trips a day in about 30 min interval (without too little variations) between both islands. An onboard data collection system records all the parameters listed in Table 1. The time series of Vg along a typical trip is shown in Fig. 3, where a one-minute moving average smooth is used to reduce measurement noises. Normally, a trip is composed three sailing stages:

- Acceleration, i.e., roughly the first 5 min at the start of a trip.
- Steady/Cruising, i.e., the ferry reaches service speed. The derivative of speed, i.e., acceleration, is used to identify the steady states along the trip. For example, the sailing history located between the two dashed lines are considered to be stead state sailing.

Table 1
Main operational parameters of double-ended ferries. *FCR: Fuel Consumption Rate.

Symbol	Feature	Units	Symbol	Feature	Units
V_g	Speed Over Ground	knots	n_s	Rotation Speed of Stern Engine	rpm
φ_{ship}	Ship Heading	deg	n_b	Rotation Speed of Bow Engine	rpm
L_s	Load of Stern Engine	%	V_{WR}	Relative Wind Speed	m/s
L_b	Load of Bow Engine	%	φ_{WR}	Relative Wind Angle	deg
m_s	FCR* of Stern Engine	l/h	V_{sc}	Sea Current Speed	m/s
m_b	FCR* of Bow Engine	l/h	φ_{sc}	Sea Current Angle (North)	deg

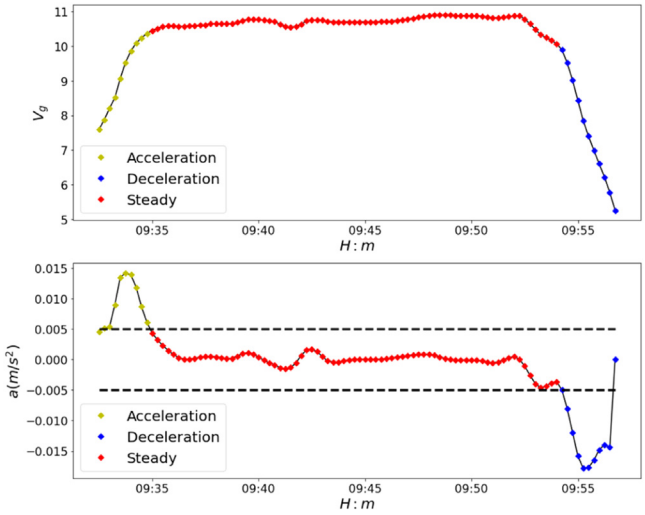

Fig. 3. Three different sailing stages in terms of speeds (upper plot), and identificaion of steady states by introducing speed acceleration (dashed lines) at the bottom plot.

- Decceleration, i.e., when the ferry is close to destination and reduces its speed.

In this study, only the steady sailing time are considered for the analysis.

2.2. Data analytics of ferry collection data

Even though ship principles indicate that ship propellers work with highest efficiency when located at the ship stern [35], how to allocate power distribution between different engines/propellers is still not clear to the operators for those double-ended ferries. In the following, let the power ratio (Rp) be used to describe the power allocation between bow and stern engines as,

$$R_P = \frac{P_{\text{stern}}}{P_{\text{bow}} + P_{\text{stern}}} \tag{1}$$

The average power allocation Rp for each trip is estimated and its distributions are presented in Fig. 4. The power allocation is almost equal distributed from 0.5 to 0.9, without significant concentration of putting most of power at the stern engine. In addition, Fig. 5 presents how the Rp affects total fuel consumption along each trip with fixed ETA. These results show good agreement with the simulations from [14], which showed that the lowest total power was observed to occur at a 100 % stern power allocation. However, the challenge for the double-ended ferry is that the information of use as much as the stern engine does not guide operators with proper settings for each engine to achieve a given the desired target speed (ETA). Fig. 5 also indicates that although the mean total fuel consumption decreases with the increments of Rp, there is no guarantee that optimal Rp always occurs at 100 % stern allocation due to other influence parameters. Therefore, this study aims at developing onboard DSS to determine the optimal set-points of both bow and stern engines by combining machine learning techniques and optimization algorithms for minimum fuel consumption.

2.3. Data-driven ship and engine performance models

Some physical or semi-empirical models are available for practical ship operations, but the physical components and corresponding coefficients inside those models were mainly established from conventional ships. They are often associated with large uncertainties even for those conventional ships, and therefore are capable of modelling the operation performance of double ended ferries. Given the availability of large volumes of data, machine learning methods become attractive to model a ship's performance more accurately. In this study, the fuel consumption of two engines and the corresponding ferry speeds are modelled by the XGBoost

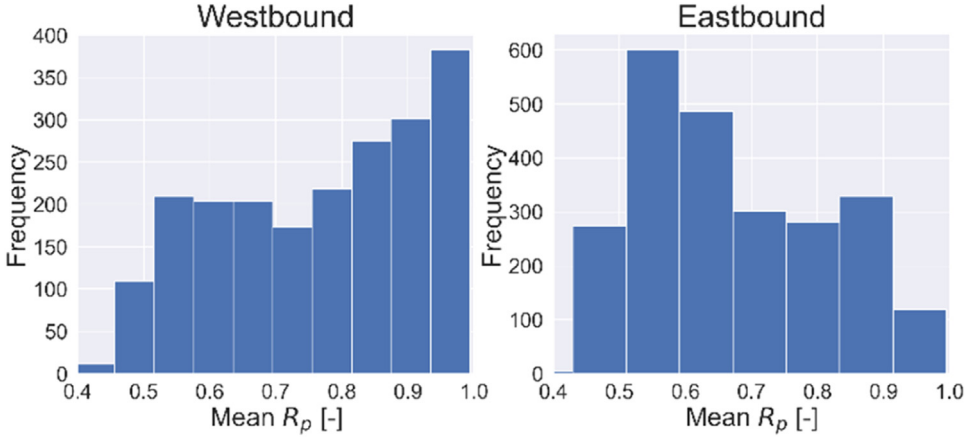

Fig. 4. Histogram of the distribution of mean engine power allocation ratio for different trips.

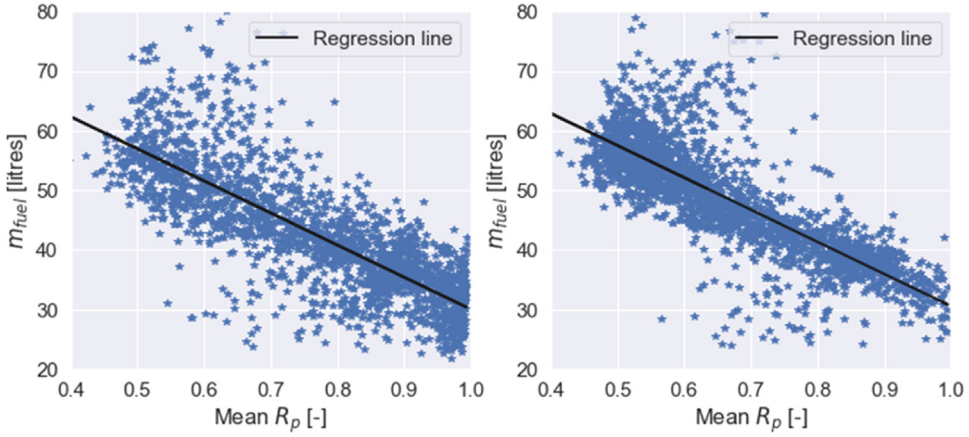

Fig. 5. Total fuel consumption in terms of mean R_p for each trip of the double-ended ferry.

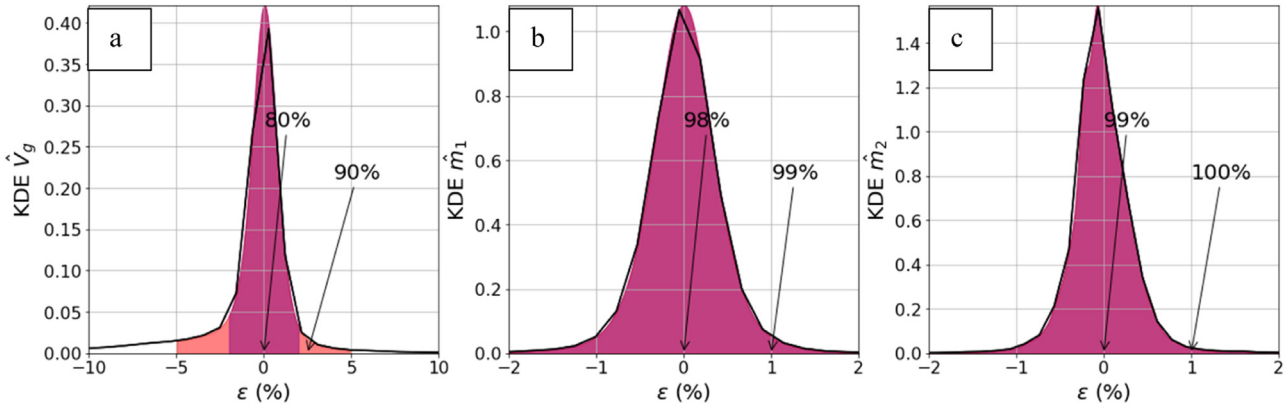

Fig. 6. Kernel distribution plot for the prediction error of the XGBoost data-driven modes: a) Fuel consumption of stern engine, b) Fuel consumption of bow engine, c) Ship speed overground. (For interpretation of the references to colour in this figure legend, the reader is referred to the web version of this article.)

method as,

$$\dot{m}_s = f_s\left(n_s,\ L_s,\ n_b,\ L_b,\ W\right)$$
$$\dot{m}_b = f_b\left(n_s,\ L_s,\ n_b,\ L_b,\ W\right)$$
$$V_g = f_v\left(n_s,\ L_s,\ n_b,\ L_b,\ \varphi_{ship},\ V_{sc},\ \varphi_{sc},\ V_{wr},\ \varphi_{wr}\right) \quad (2)$$

where W denotes all ocean weather related parameters, and the other parameters are described in Table 1, and they are chosen as the features of those models because they are acting as either the control variables or constraints of the decision-making system. Before such data-driven ship performance models integrated into the proposed DSS here, the model accuracy was assessed by the coefficient of determination R^2. The two models developed for fuel consumption demonstrated high accuracy with an R^2coefficient of 0.9999, i.e., almost deterministic results. The ship speed resulted in an R^2coefficient of 0.945, also indicating very accurate predictions. The reason R^2 of speed is lower than fuel is the fact it is impossible to consider/collect all speed related features in the data-driven models. To further evaluate the accuracy of the models a kernel density estimate (KDE) was fitted to model the distribution of the prediction error ϵ, which is presented in Fig. 6. The KDE shows that both *ms* and *mb* models have very high accuracy, with approximately 99 % of the errors falling within the range of ±1 %. While more than 90 % of the errors fall in the range of 5 % for the speed prediction.

Furthermore, the prediction of a typical trip (collected July 2022) with sailing speed Vg of 10.42 knots and a recorded fuel consumption of f_{fuel}=32 *l* is also used to show the model accuracy. The input features of measurements from this trip are presented in Fig. 7 (left), where the stern engine has constant speed at 1258 rpm and the bow engine presents two setpoints during the steady operation. As shown in Fig. 7 (right), the data-driven speed model can perfectly predict well the measured speed, while the fuel consumption models of both stern and bow engines give perfect prediction results in comparison with the measurements. The prediction accuracy quantified by the mean errors of prediction in percentages along the entire trip, for the speed is of 0.78 % discrepancy, and 0.16 % and 0.28 % for fuel consumption rates of stern and bow engines. Therefore, those data-driven models could be reliably used in the Bayesian optimization method for the proposed DSS in this study.

3. Methods in the decision support system

The flowchart and methods for the proposed DSS of double-ended ferries are presented in Fig. 8 to determine optimal operational set-point parameters/inputs of a specific trip, i.e., an input layer of all necessary information about the trip, data-driven models required to describe the ship and engine performance, and Bayesian optimization algorithm with prior belief from proper/historical trip settings[36]. The accuracy of the proposed XGBoost machine learning method to establish data-driven ship performance models is briefly presented in Section 2.3. For the DSS working onboard, the optimization algorithm integrated should be computational efficient. Therefore, the Bayesian algorithm that can utilize prior sailing experiences/data is proposed to fulfil such requirements.

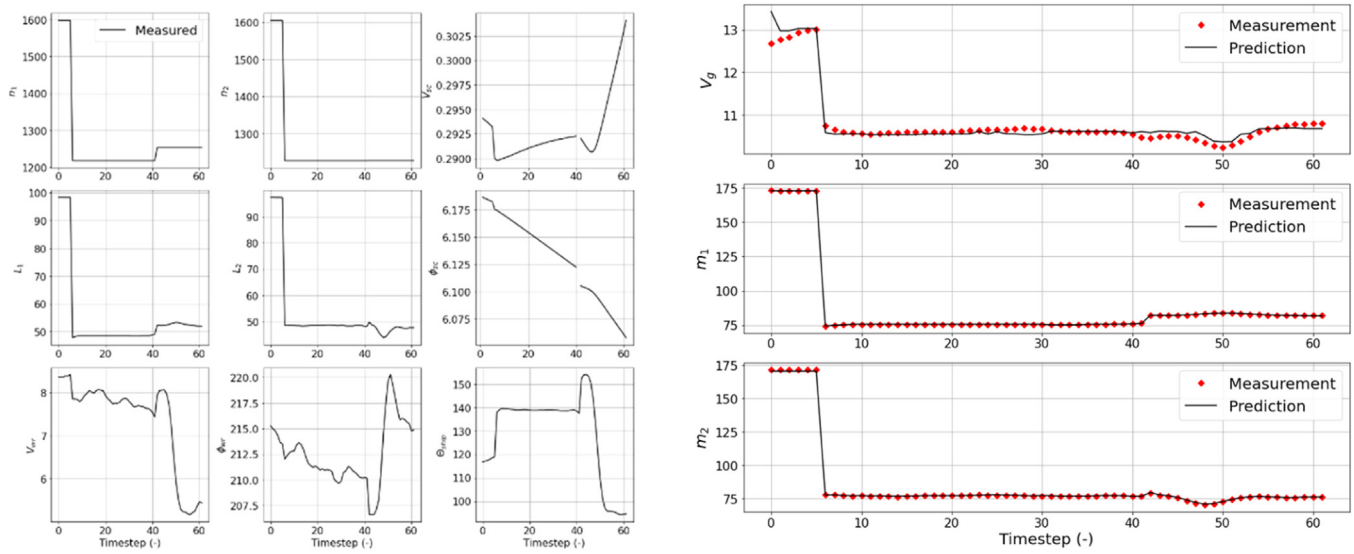

Fig. 7. Input features to the data-driven models for a typical trip of July 2022 (left), performance of the data-driven models on the trip (right).

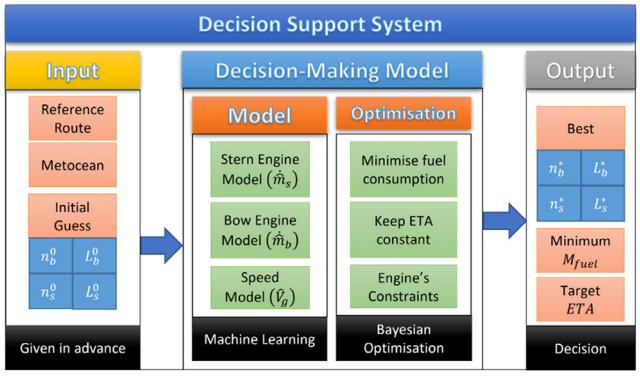

Fig. 8. The flowchart and method components of the proposed Decision Support System (DSS).

First, the ***input Layer of the DSS*** includes both prior, current, and forecast information related to the specific trip for its DSS. They serve as the interface and fed into the decision-making model as in Fig. 7.

- ***Reference route.*** It provides historical sailing waypoints (longitudes, latitudes, heading angles, etc.) similar to this trip, as well as speed *Vg* and fuel consumption.
- ***MetOcean data.*** It is extracted from the weather forecasting database. Once the route coordinates are set, and the trip schedule is known the data is interpolated to match the position and times.
- ***An initial guess or prior of "pre-assumed" optimal operation parameters.*** This optimization initialization guides the optimizer into a search space that is most likely to contain stationary points that allow for the reduction of fuel consumption.

3.1. Optimization framework in DSS

The task of the proposed DSS is to find optimal control parameters for a double-ended ferry's operation, i.e., the engine load and rotation speed of both stern and bow engines $\boldsymbol{\xi} = [Ls,\ Lb,\ ns,\ nb]$, respectively. These control parameters can be easily set on the ferry's bridge platform. For a specific trip, its actual operation is normally divided into several sailing legs. A ship's operational control parameters are fixed along each sailing leg. Since double-ended ferries are normally sailing as commuters of short distance/time, it is enough to treat an entire trip as a sailing leg. Therefore, the proposed DSS for the double-ended ferry is to find optimal values of those control parameters for the entire trip that can fulfil the following objective, i.e., to minimize fuel consumption,

$$J\left[L_s^*, L_b^*, n_s^*, n_b^*\right] = \underset{L_s,L_b,n_s,n_b}{\arg\min} \left(f_{fuel}\right) \text{for a fixed sailing time } Ts \tag{3}$$

where f_{fuel} is the cost function of total fuel consumption along the given trip. It can be computed by integration of the instantaneous fuel consumption m_s, m_b from the above data-driven models as,

$$f_{fuel} = \int_0^{T_s} \left(\dot{m}_s + \dot{m}_b\right) dt = \sum_{i=1}^{n} \left(f_s(n_s,\ \ n_b,\ L_s,\ L_b,\ W_i) + f_b(n_s,\ \ n_b,\ L_s,\ L_b,\ W_i)\right) \Delta T_i \tag{4}$$

where ΔT_i is the time interval of data collection, e.g., 1 min in this study. For the entire trip, the total sailing time of searching candidate routes may differ from the initial prior/reference route even assuming the same trajectory, while another optimization objective is to minimize the difference,

$$J_{time} = \underset{L_s,L_b,n_s,n_b}{\arg\min} (T_s^{opt} - T_s),\ \text{ with } T_s^{opt} = T_s \cdot \frac{\bar{V}_g^{ref}}{\bar{V}_g^{opt}} = \sum_{i=1}^{n} \Delta T_i. \tag{5}$$

To make the optimization process converge fast, the time objective is treated as constraints allowing a relative tolerance range of $\pm\ q\%$. Together with the engine operation constraints, the full set of constraints for the optimization problem are defined as follows,

$$\begin{cases} 0 \le L_{s,b} \le L^{max} \\ 0 \le n_{s,b} \le n^{max} \\ \left|1 - \frac{T_s}{T_s^{search}}\right| = \left|1 - \frac{\bar{V}_g^{search}}{\bar{V}_g^{ref}}\right| \le q\% \end{cases} \tag{6}$$

where the average speed from searching candidate routes $\bar{V}_g^{search}$ can be estimated by the data-driven models in Eq. (2). For the DSS in this study, the tolerance of actual ETA is chosen as 5 %. To solve the above objective functions of three black-box models, gradient-free optimization algorithms are needed. For example, the Grid Search, a brute force algorithm (Feurer and Hutter, 2019), divides the searching domain into grids, then evaluates the objective function and the constraints on each grid. This can be extremely slow and computationally expensive. In this study, the Bayesian

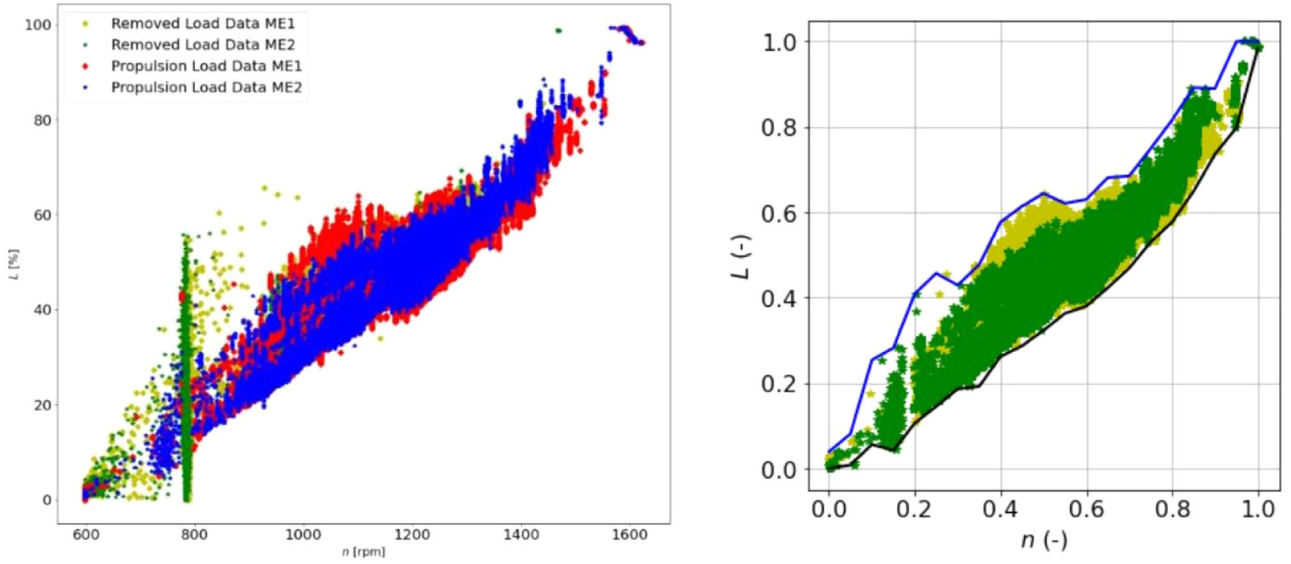

Fig. 9. Samples of engine control settings (left), the scaled upper and lower boundaries to define proper $L-n$ search space (right).

Table 2
Algorithm 1 - *Determination of "prior" parameters for the BP model in Bayesian method.*

Algorithm 1 – *Determination of "pre-assumed" optimal operation parameters*

1: Load the historical data.
2: Specify the intended trip's Direction and V_g
3: Split R_p in k evenly distributed intervals between 0.4 and 1.0.
4: Specify a tolerance value for ΔV_g and ΔR_p (e.g. 5 %)
5: Filter the data by Direction and by $V_g \pm \Delta V_g$
6: For each of the k-1 splits of R_p apply an additional filter of $R_p \pm \Delta R_p$
7: Compute the mode of $f(n_b,\ L_b,\ n_s,\ L_s)$ and record the values of $n_b,\ L_b,\ n_s,\ L_s$
8: Repeat 6 and 7 until all values are recorded.
9: Remove any duplicate values for the quads $n_b,\ L_b,\ n_s,\ L_s$ if existing.

optimization is used to accelerate the optimization process. It is an iterative algorithm, and every iteration keeps track of the information from the previous evaluation to explore the search space $D(L, n)$ allowing to convergence in a relatively low number of iterations (Nogueira, 2014).

3.2. Refinement of search space ξ

The searching space of the engine setpoints $\zeta(L,n)$ in the optimization process is constraint to the area presented in Fig. 9 according to their practical operations. First, the L-n band corresponding to the range 775 to 795 rpm Fig. 9 (left) was removed from the dataset because of very little data and measurement noises. The reserved setpoints are scaled in the range [0 1] to define the constraints in the nondimensional space. It shows that the engine's load could be modelled in terms of the engine speed. Simple piecewise polynomials are used to define the constraints, i.e., minima and maxima of L, as

$$\begin{cases} L_i^{\max}(n_i) = a_0 + a_1 \cdot n_i + a_2 \cdot n_i^2 + a_3 \cdot n_i^3 \\ L_i^{\min}(n_i) = b_0 + b_1 \cdot n_i + b_2 \cdot n_i^2 + b_3 \cdot n_i^3 \end{cases} \tag{7}$$

where the coefficients a_j, b_j are estimated by using ordinary least squares.

Furthermore, Fig. 5 indicates that there is a trend towards higher use of the stern engine on the operation probably mainly for ETA purposes. To account for this effect the search space is further refined. This serves to further guide the optimization process into a space of control inputs for fast convergence and allowing for real-time planning. The optimal operation setpoints are also expected to locate in the reduced search space given by,

$$\begin{aligned} n_{\text{stern}} &= [0.45, 1] L_{\text{stern}} = [0.45, 1] \\ n_{\text{bow}} &= [0, 0.55] L_{\text{bow}} = [0.45, 1] \end{aligned} \tag{8}$$

3.3. Bayesian optimization ingredients

The above cost function is not particularly difficult to evaluate but determining its minimum/optimal objective value can be tricky. In the Bayesian optimization algorithm of the DSS, the Gaussian Process (GP) model is chosen to describe the prior probability model, also called surrogate model to approximate the objective function. And the prior samples are selected from the ferry's previous navigations by the Algorithm 1 presented in Table 2, based on the target trip's pre-defined sailing characteristics from the input layer. Let the selected k trips denote by $D_k = (\xi_1, f_{\text{fuel }1}), \ldots, (\xi_k, f_{\text{fuelk}})$. In this study, the Matern kernel is used to describe the covariance function $\mathbf{\Sigma}_{k\times k}$ of the GP model,

$$\mathbf{\Sigma}_{i,j} = \text{Cov}\left(\xi_i, \xi_j\right) = \sigma^2 \frac{2^{1-\nu}}{\Gamma(\nu)} \left(\sqrt{2\nu} \frac{\xi_i - \xi_j}{\rho} \right)^{\nu} K_\nu \left(\sqrt{2\nu} \frac{\xi_i - \xi_j}{\rho} \right), \tag{9}$$

where $\Gamma(-)$ is a gamma function, $K_\nu(-)$ is a Bessel function, $\nu = 2.5$ in this study, and other parameters can be regressed from the data samples D_k. For any new input control parameter ξ_{k+1}, the GP surrogate model can give us the predictive distribution of $f_{fuel}(\xi_{k+1})$, i.e., normal distribution as,

$$f_{\text{fuel}}\left(\xi_{k+1}\right) \mid D_k \sim N\left(\mu\left(\xi_{k+1}\right), \sigma^2\left(\xi_{k+1}\right)\right), \tag{10}$$

Table 3
verification of DSS for historical trips based on performance simulations.

Direction	Trip case no.		Measurements		Optimization		Change
			M_{fuel} (l)	R_p	M^*_{fuel} (l)	R^*_p	V_g (%)
Westbound	W1	2021–10–14 19:30	45.12	0.472	25.45	0.898	+1.44 %
	W2	2021–07–05 08:10	40.08	0.549	25.21	0.947	+0.40 %
	W3	2021–10–23 19:45	39.78	0.480	35.62	0.523	+0.07 %
Eastbound	E1	2021–05–26 08:45	33.48	0.565	28.47	0.684	+1.39 %
	E2	2021–09–06 14:50	31.93	0.649	23.11	0.958	+1.8 %
	E3	2021–08–06 10:45	29.11	0.535	18.73	0.624	+0.44 %

with the following mean and variance,

$$\mu\left(\xi_{k+1}\right) = \mathbf{\Sigma}\left(\xi_{k+1}, \xi_{1,\ldots,k}\right)\mathbf{\Sigma}_{k\times k}^{-1} f_{fuel}\left(\xi_{k+1}\right)$$
$$\sigma^2\left(\xi_{k+1}\right) = 1 - \mathbf{\Sigma}\left(\xi_{k+1}, \xi_{1,\ldots,k}\right)\mathbf{\Sigma}_{k\times k}^{-1}\mathbf{\Sigma}\left(\xi_{k+1}, \xi_{1,\ldots,k}\right)^T \quad (11)$$

where $\mathbf{\Sigma}(\xi_{k+1}, \xi_{1,\ldots,k}) = [\mathrm{Cov}(\xi_{k+1}, \xi_1), \mathrm{Cov}(\xi_{k+1}, \xi_2), \ldots, \mathrm{Cov}(\xi_{k+1}, \xi_k)]$. To find the next iteration operational set-points ξ^*_{k+1} in the search space D, an acquisition function is needed in the optimization. In this study, the Negative Lower Confidence Bound (NLCB) based on the famous upper confidence bound bandit strategy is adopted as,

$$\xi^*_{k+1} = \mathrm{argmax}_{\xi_{k+1}} u\left(\xi_{k+1}\right) = \mathrm{argmax}_{\xi_{k+1}}\left(\mu\left(\xi_{k+1}\right) - \beta\cdot\sigma\left(\xi_{k+1}\right)\right), \quad (12)$$

where the hyperparameter is defined as $\beta = 2.576$ corresponding to 99 % Type equation here. confidence interval, which is used to balance the trade-off between exploration and exploitation.

After finding the next iteration set-points ξ^*_{k+1}, the data-driven models Eq. (2) estimate the objective function. The new sample $(\xi^*_{k+1}, f_{\mathrm{fuel}}\ (\xi^*_{k+1}))$ together with previous samples to form the new prior sample space as D_{k+1}. Finally, the entire process will repeat until it converges to the optimal solutions.

4. Results of DSS for the double-ended ferry

Both ship performance simulation-based verification and full-scale test results are carried out to evaluate the effectiveness of the DSS for the case study double-ended ferry. In the simulation-based verification, 3 westbound and 3 eastbound trips are chosen randomly, and they are expected to represent overall operation cases observed in the dataset. In addition, full-scale tests were performed onboard this ferry for about 3 days, where some trips were guided by the DSS and some were not by intention.

4.1. Verification of DSS for historical trips on ship performance simulations

When applied the DSS for the 6 chosen representative trips, their sailing route (trajectory, average speed and ETA) are assumed to be the same as the measurements. In addition to the trip related inputs fixed as the measurement, the surrounding ocean environment along the trip may differ slightly depending on the speed profile along the trip from the optimization process. Finally, the decision-making optimizer finds the most proper control inputs of ns, nb, Ls, Lb, which are recognized as the optimal operation for this trip based on the DSS ensuring the same ETA. Since the Bayesian optimization in the DSS will require huge amounts of iterations to get “exact” ETA as measured, 2 % tolerance of average speed differ is set to assume the same ETA.

The overall results and their improvement of fuel saving by implementing this DSS are presented in Table 3. It can be observed that significant fuel savings can be achieved by the DSS with little discrepancy of ETA (average speed) for all the simulated trips. The main reasons of the fuel saving can be contributed by trying to push the propulsion power to the stern engine as much as possible. The smallest fuel saving is for the westbound W3 trip. It is because it is not enough to ensure ETA by only using the stern engine, a lot of propulsive power must also be required from the bow engine. More equally distributed allocation of bow and stern engine, i.e., Rp, can be also observed frequently in eastbound trips, because they were normally running fast to catch up road transport for people onboard. The optimizer in the DSS tried to put power on both engines. But due to wind and ocean currents often blow from the west to the east, their total fuel consumption is normally lower than westbound trips. To give some details of the Bayesian optimization in the DSS, one westbound trip W1 and one eastbound trip E2 are chosen to be presented regarding their operation along the trip.

4.1.1. A westbound trip

First, to show the performance simulation using the data-driven models can reflect the actual characteristics of the ferry’s performance, the speed profile, fuel consumption at bow and stern engines along the trip are estimated by the established data-driven models. Their results are presented in Fig. 10 (left), which shows that the data-driven models can properly model the ferry performance for this trip. Then, those data-driven models can be used in DSS for control inputs setting. Relevant results of speed and engine fuel consumptions after the optimization in DSS are presented in the right plot. The optimized trip has less than 2 % change in their target average speed respect to the original ETA. Higher tolerance may be beneficial to have even better ETA but take long time to reach convergence. This parameter can be manually set. The DSS can lead to 43 % fuel reduction compared to the original trip.

The optimal set-points of *nb, Lb, ns, Ls*, are presented in Fig.11. The optimal condition shows that the power demand is increased on the stern engine and greatly reduced on the bow engine. Under these new setpoints the ship that originally sailed at an average speed of 9.43 knots now sails 9.57 knots or a 1.43 % increase in speed and a similar reduction in ETA. The optimum set point reallocates the load and speed between engines to increase the overall trip’s efficiency.

4.1.2. An eastbound trip

Similar results can be observed on the eastbound trip E2 as in Fig. 12, which presents only the optimized performance (left) and engine settings (right), because the data-driven models have been validated enough by previous sections. The trip again shows a drastic reduction in *nb, Lb* with a consequent increase in *ns, Ls* The trip has an increase in speed of 1.8 % going from an original speed of 9.82 knots to 10.0 knots in average.

It should be noted that these results might be a bit overoptimistic from the simulation. For example, a ferry may be difficult to always keep constant engine settings along the entire trip, even though this constant power settings have been reported by many researchers of highest energy efficiency. In the following, the DSS optimized engine settings will be given to ferry operators, who will

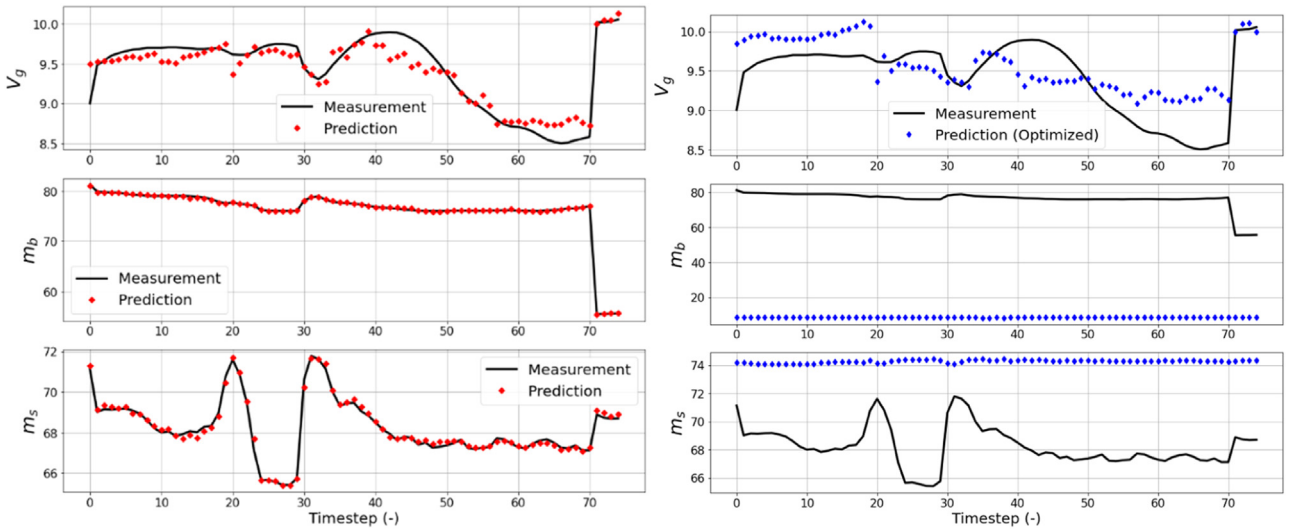

Fig. 10. Prediction of the operation performance by the XGBoost data-driven models using the original trip set-points (left), the corresponding results after the trip optimization in DSS (right) for the trip W1. (For interpretation of the references to colour in this figure legend, the reader is referred to the web version of this article.)

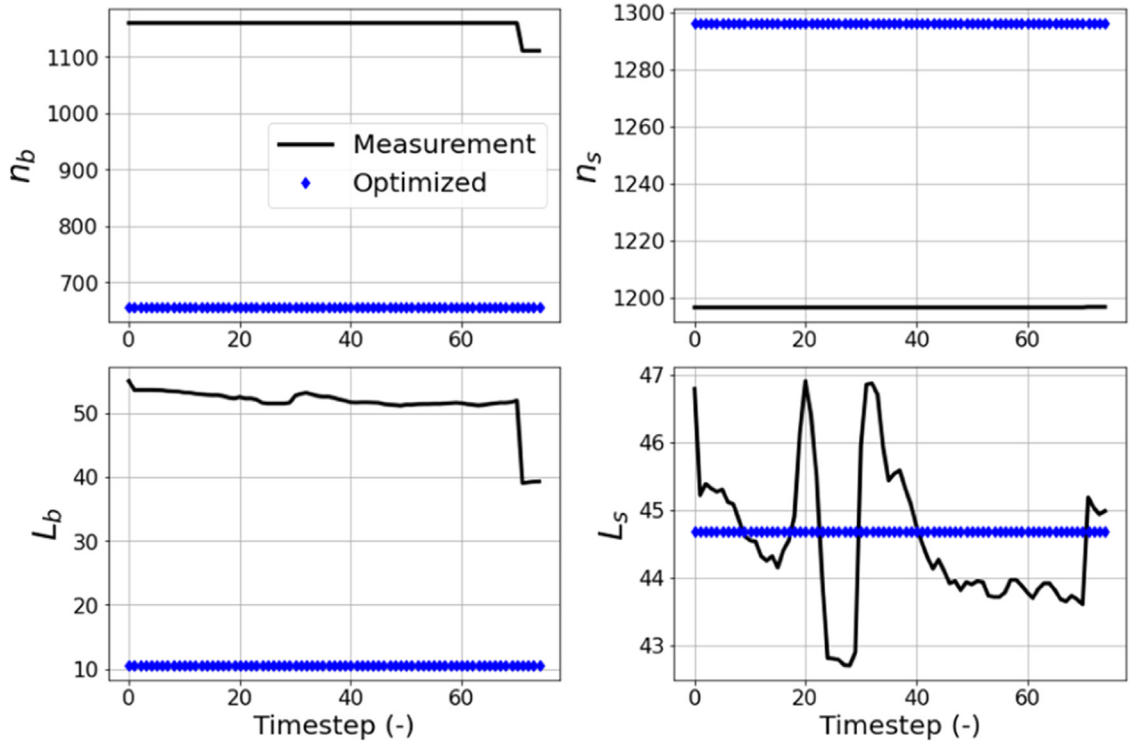

Fig. 11. Optimal setpoints for the trip W1 estimated by the proposed DSS.

try to follow the guided setting as close as possible for their full-scale experiments/operations.

4.2. Full-scale test results for actual ferry operations

The full-scale tests were conducted between August 19 and August 22 of 2022 onboard the ferry to infer the effects of simple power allocation on fuel consumption. The experiment was designed so that the ferry was operated by either the captain or the 1st Mate every other round trip. The captain was instructed before the experiment to operate the ferry by allocating most of the power at all times on the stern thruster. The 1st Mate was unaware of the experiment and was expected to operate with a normal power allocation. Round trips were initiated at 1–2 h intervals to ensure that the captain and the 1st Mate encountered conditions as consistently as possible during the experiments, particularly concerning weather and traffic scenarios. Fig. 13 illustrates the fuel consumption throughout the entire voyage as a function of R_p, and Fig. 14 presents the accuracy of data-driven models to predict the ferry's operational performance, i.e., speed, fuel consumption at both engines. The observed trend aligns with that from previous data analysis. To have a fair comparison, some trips were filtered out if their mean speed (ETA) differs significantly from normal operations. Fig. 13 (right) indicates the

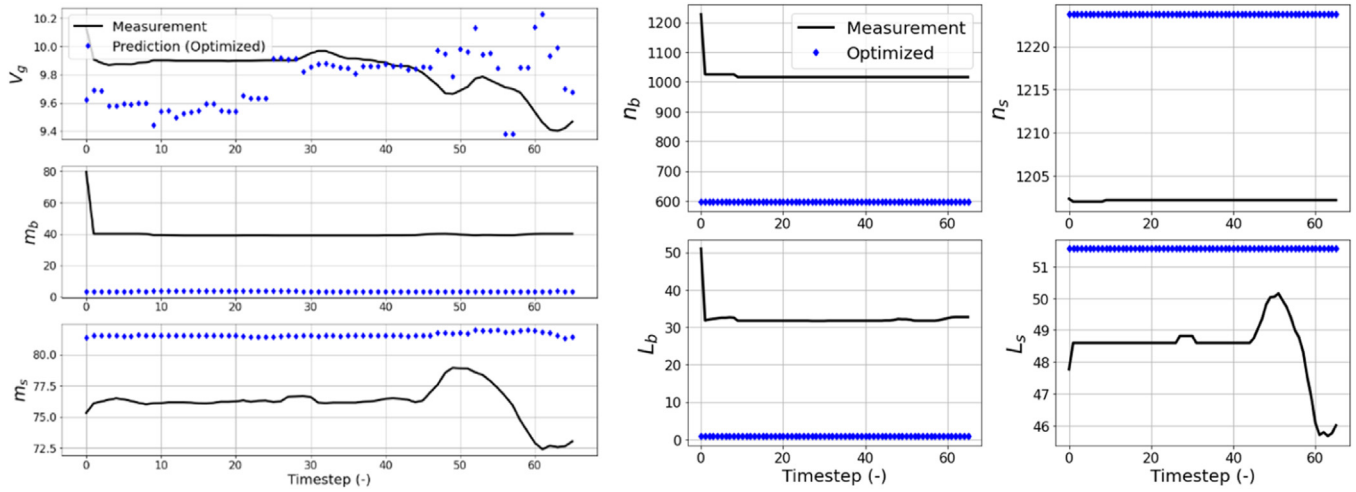

Fig. 12. Optimized speed and two engine performance (left), and optimal setpoints (right) for the chosen eastbound trip EW1 estimated by the proposed DSS.

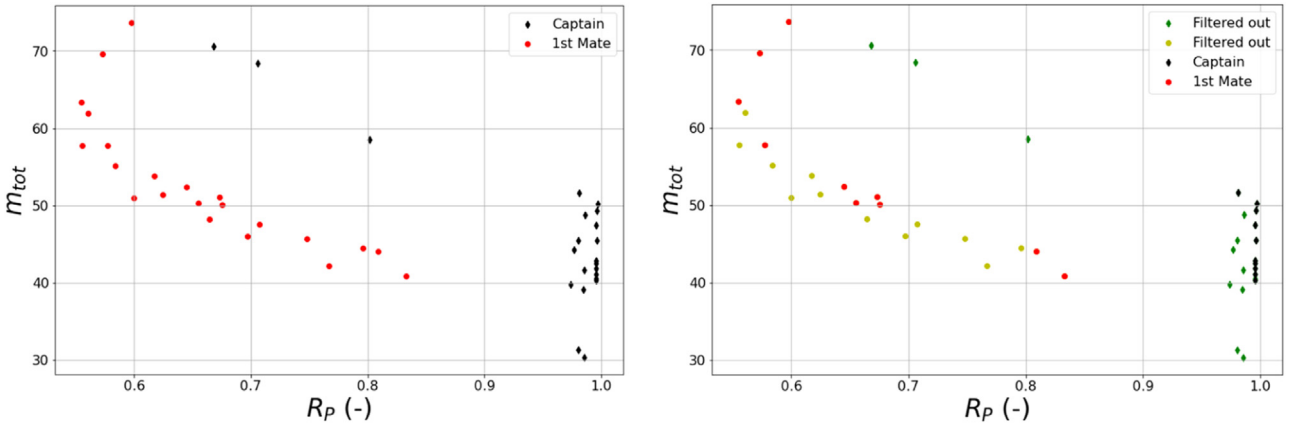

Fig. 13. Total fuel consumption vs power allocation R_p for different trips, all test trips without filtering (left), filtering of trips based on speed/ETA difference (right).

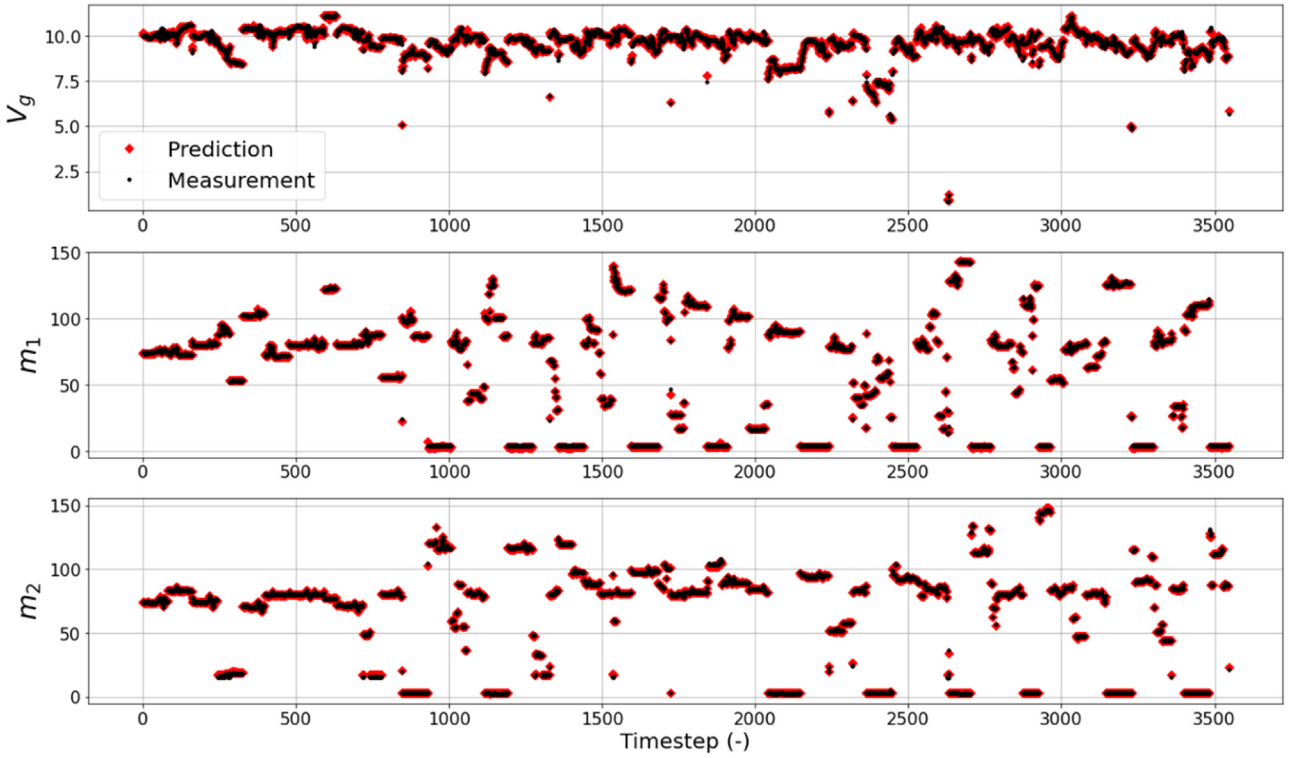

Fig. 14. Forecasting of the XGBoost data-driven models on the full-scale test data.

Table 4
Summary of the full-scale test results.

Operator	Period	Number of valid trips	V_g (knots)	R_p	M_{fuel}
1st Mate	Reference	10	9.3	0.7	57
Captain	Reference	10	9.3	0.8	53
1st Mate	Experiment	10	9.4	0.7	55
Captain	Experiment	10	9.5	1.0	45

number of trips filtered out due to their either too high or too low speeds. After filtering 10 trips for each operation modes (i.e., Captain vs 1st Mate) are considered for the analysis.

A reference period, preceding the experimental phase, was rigorously analysed to discern any disparities in the operational experiences of the captain and the 1st Mate prior to the experiment. During this reference period, the captain and the 1st Mate alternated in operating the ship every subsequent round trip, adhering to an identical schedule as that of the experimental phase. Table 4 encapsulates the comparative analysis of round trips managed by the captain and the 1st Mate across both the reference and experimental periods. Remarkably, the captain exhibited a consistently reduced fuel consumption relative to the 1st Mate across both intervals. Notwithstanding the captain's marginally elevated aft thruster utilization before the experiment (0.8 in contrast to 0.7), alternative factors might contribute to the captain's diminished consumption, including superior expertise and adeptness in ship operation. Intriguingly, the disparity in consumption was considerably accentuated during the experiment (18 %) as opposed to the reference period (8 %). Prior to the experimental phase, the captain's aft thruster utilization was measured at R_p=0.8, which escalated to an exclusive use (R_p =1.0) during the experiment. This suggests that a minimum of 10 % from the total 18 % reduction can be attributed to the augmented aft thruster utilization. The residual variance in fuel consumption between the captain and mate during the experiment (8 %) might emanate from other operational optimization avenues, warranting comprehensive investigations beyond the purview of this study.

5. Conclusion

This study provides with a Decision Support System that allows for a better operation of double-ended ferries. It provides with a method to optimize the control inputs of a double ended ferry to minimize fuel consumption. The operation was simplified to a constant engine's speed and load. The DSS combines data-driven models, which are established to predict the ship's speed and fuel consumption at both bow and stern engines, and the Bayesian optimization algorithm. In the Bayesian optimization method, similar trips to the planning trip are chosen to get the prior model. Furthermore, some practical operational constraints are also derived from data analysis to refine the searching space of the Bayesian optimizer. Both example trips from both the original dataset and actual full-scale tests are performed to verify the optimal engine setting obtained by the proposed DSS.

For the historical example trips, the data-driven models are used to simulate a ship's performance, such as speed and fuel consumptions. First, the data-driven models give perfect prediction of fuel consumption at both engines. The prediction of ship speed is also good enough for the application of DSS. The optimized solutions show that a reduction of fuel consumption of up to 40 % in comparison with the historical/original operations in the dataset, as well as less than 2 % error in the ETA. For the full-scale tests, the DSS guided stern power allocation contributes to about 18 % average fuel savings. Finally, it is concluded that allocating more power in the stern engine can help to reduce fuel consumption of double-ended ferries. The precise optimal power allocation between bow and stern engine also depends on the target ETA and engine capacity. It can be obtained by the proposed Decision Support System, which also relies on good performance input models for a general double-ended ferry.

Declaration of Competing Interest

This paper is our original unpublished work and it has not been submitted to any other journals for reviewing. Hereby, we would like to declare that we have no conflict of interest with any other researchers.

Acknowledgements

The authors acknowledge the financial support from the Vinnova project 2021–02768 and the sustainable shipping program from Lighthouse/Trafikverket (Swedish Transport Administration). We are also grateful to the support from the Swedish Foundation for International Cooperation in Research and Higher Education (CH2016–6673).

References

[1] IMO, Resol. MEPC 304 (72) (2018).
[2] IMO, Resol. Mepc 346 (78) (2022).
[3] H. Wang, W. Mao, L. Eriksson, Ocean Eng. 186 (2019) 106131.
[4] H. Wang, X. Lang, W. Mao, Transp. Res. D Transp. Environ. 90 (2021), doi:10.1016/j.trd.2020.102670.
[5] Wang, H., Lang, X., Mao, W., Zhang, D., Storhaug, G., 2020. Ocean Eng.. 200, 107063. doi:10.1016/j.oceaneng.2020.107063.
[6] V. Jaramillo, H. Kim, Z.H. Munim, J. Clean. Prod. 366 (2022) 132888, doi:10.1016/j.jclepro.2022.132888.
[7] X. Lang, D. Wu, W. Mao, Ocean Eng. 245 (2022) 110387, doi:10.1016/j.oceaneng.2021.110387.
[8] F.H. Berthelsen, U.D. Nielsen, Transp. Res. D Transp. Environ. 99 (2021) 102996, doi:10.1016/j.trd.2021.102996.
[9] C. Gkerekos, I. Lazakis, G. Theotokatos, Ocean Eng. 188 (2019) 106282, doi:10.1016/j.oceaneng.2019.106282.
[10] D. Kim, S. Lee, J. Lee, Sensors 20 (6) (2020) 1588, doi:10.3390/s20061588.
[11] Y.R. Kim, M. Jung, J.B. Park, J. Mar. Sci. Eng. 9 (2) (2021) 137, doi:10.3390/jmse9020137.
[12] P. Theodoropoulos, C.C. Spandonidis, N. Themelis, C. Giordamlis, S. Fassois, J. Mar. Sci. Eng. 9 (2) (2021) 116, doi:10.3390/jmse9020116.
[13] Yrjänäinen, A. et al., (2019). In Papanikolaou, A. (Ed.), A Holistic Approach to Ship Design: Volume 1: Optimisation of Ship Design and Operation for Life Cycle. (pp. 76–113). Springer International Publishing. doi:10.1007/978-3-030-02810-7_4.
[14] Jokinen, M. et al. (2021). In Papanikolaou, A. (Ed.), A Holistic Approach to Ship Design: Vol 2: Application Case Studies. (pp. 394–398). Springer International Publishing. doi:10.1007/978-3-030-71091-0.
[15] D. Vergara, et al., ISOPE (2023).
[16] T.E. Berg, Ø. Selvik, K. Steinsvik, D. Leinebø, TransNav. Int. J. Marine Navig. Saf. Sea Transp. 15 (1) (2021) 63–69, doi:10.12716/1001.15.01.05.
[17] S. Li, C. Xu, J. Liu, B. Han, Ocean Eng. 273 (2023) 113994, doi:10.1016/j.oceaneng.2023.113994.
[18] M. Gianni, V. Bucci, A. Marinò, Procedia Comput. Sci. 180 (2021) 754–763, doi:10.1016/j.procs.2021.01.323.
[19] S.A. Mansouri, H. Lee, O. Aluko, Transp. Res. E Logist. Transp. Rev. 78 (2015) 3–18, doi:10.1016/j.tre.2015.01.012.
[20] P. Holptrom, J.R. Menen, Soc. Nav. Archit. Mar. Eng., Trans. 90 (1982) 62–75.
[21] U. Hollenbach, Int. Shipbuild. Prog. 45 (438) (1998) 71–76.
[22] K. Hiekata, Z. Zhao, J. Mar. Sci. Eng. 10 (2) (2022) 263, doi:10.3390/jmse10020263.
[23] A.M. Bassam, A.B. Phillips, S.R. Turnock, P.A. Wilson, Ocean Eng. 245 (2022) 110449, doi:10.1016/j.oceaneng.2021.110449.

[24] S. El Mekkaoui, L. Benabbou, S. Caron, A. Berrado, J. Mar. Sci. Eng. 11 (1) (2023) 191, doi:10.3390/jmse11010191.
[25] N. Bialystocki, D. Konovessis, J. Ocean Eng. Sci. 1 (2) (2016) 157–166, doi:10.1016/j.joes.2016.02.001.
[26] X. Lang, D. Wu, W Mao, Expert Syst. Appl. Part A 238 (2024) 121877, doi:10.1016/j.eswa.2023.121877.
[27] Dai, X., Sheng, K., Shu, F., School of Electronics and Information, Jiangsu University of Science and Technology, Zhenjiang 212003, China, Jiangsu Institute of Automation, Lianyungang 222000, China, & Zhoushan Jiangke Ship and Marine Engineering Equipment R & D Center, Zhoushan 316021, China. (2022). Ship power load forecasting based on PSO-SVM. Mathematical Biosciences and Engineering, 19(5), 4547–4567. doi:10.3934/mbe.2022210.
[28] A. Laurie, E. Anderlini, J. Dietz, G. Thomas, Ocean Eng. 234 (2021) 108886, doi:10.1016/j.oceaneng.2021.108886.
[29] J.B. Lee, M.I. Roh, K.S. Kim, Int. J. Naval Archit. Ocean Eng. 13 (2021) 641–649, doi:10.1016/j.ijnaoe.2021.08.001 .
[30] A.I. Parkes, A.J. Sobey, D.A. Hudson, Ocean Eng. 166 (2018) 92–104, doi:10.1016/j.oceaneng.2018.07.060.
[31] M. Abebe, Y. Shin, Y. Noh, S. Lee, I. Lee, Appl. Sci. 10 (7) (2020) 2325, doi:10.3390/app10072325.
[32] A.M. Bassam, A.B. Phillips, S.R. Turnock, P.A. Wilson, Ocean Eng. 278 (2023) 114613, doi:10.1016/j.oceaneng.2023.114613.
[33] F. Cipollini, L. Oneto, A. Coraddu, A.J. Murphy, D. Anguita, Ocean Eng. 149 (2018) 268–278, doi:10.1016/J.OCEANENG.2017.12.002.
[34] A. Coraddu, L. Oneto, F. Baldi, D. Anguita, Ocean Eng. 130 (2017) 351–370, doi:10.1016/j.oceaneng.2016.11.058.
[35] Larsson, L., & Raven, H. (2010). (1st ed.). The Society of Naval Architects and Marine Engineers (SNAME).
[36] J. Bergstra, Y Bengio, J. Mach. Learn Res. 13 (2012) 281–305.